Proceedings of Global Power and Propulsion Society
ISSN-Nr: 2504-4400
GPPS Xi'an21
18th – 20th October, 2021
www.gpps.global

GPPS-TC-2021-0057

Research on the Aero Design System for the Ultra-Highly-Loaded Aspirated Fan

Lei Wang
Xi'an Shaangu Power Co.,Ltd
Wl006903@shaangu.com
Xi'an, ShaanXi, China

Bo Liu
Northwestern Polytechnical University
Liubo704@nwpu.edu.cn
Xi'an, ShaanXi, China

ABSTRACT

Each design steps in the aspirated design method are discussed in detail, through comparison with the conventional aerodynamic design system, the uniqueness of each design link after the use of boundary layer suction technology is summarized. The essence of the MIT aspirated design method is extracted, and its shortcomings are improved, and a relatively complete adsorption design method was initially established. The design of an adpirated fan with a stage pressure ratio of 3.5 and a load factor of more than 0.7 is completed. The suction hole is simulated in the form of the addition of the source term, and the non-linear harmonic method that takes into account the unsteady effect is used for full three-dimensional analysis and verification. By incorporating the boundary layer suction concept into the through-flow and blade design stages, a peak efficiency of 85.34% and a peak pressure ratio of 3.55 can be achieved using only 1.5% of the suction capacity.

INTRODUCTION

Currently, an important development direction of compressor design is to continuously improve the stage pressure ratio. There are two main ways: increasing the tangent speed of the blade and increasing the turning angle of the blade. However, the increase of the rotor speed is not only limited by the maximum stress that the blade can withstand but also increases the shock wave loss itself and a series of losses induced by the shock wave. Likewise, the design method of increasing the turning angle of the blades to achieve a higher pressure ratio is also limited by flow separation. Therefore, how to effectively control the separation of the boundary layer is a key technology to improve the performance of the compressor. In order to control the separation of the boundary layer of the suction surface, Kerrebrock [1] proposed the concept of an aspirated compressor in 1997, and his subsequent research further showed that after the use of boundary layer suction technology, the compressor's diffusion capacity far exceeds compressor with conventional aerodynamic layout. Since 1998, Merchant et al. [3-8] successively designed two aspirated fans and aspirated counter-rotating fans, one with a low-pressure ratio and low tangential speed, anpther with a high-pressure ratio and high tangential speed. In recent years, China has also begun to pay attention to the technical development of aspirated compressors. In the previous literature [9], the highly-loaded compressor cascades are applied to explore the effect of different suction positions of endwall upon the flow structure of the corner region and passage vortex developing process. The study showed that the suction location of the 25% chord endwall after the shock of the cascade channel can elimate the high-entropy low-energy air flow accumulated on the upstream end wall, limit the development of the passage vortex, and improve the flow field structure of the cascade channel. Literature [10] takes the transonic fan rotor ATS-2 as the research object and performs a fully three-dimensional numerical simulation of surface layer suction at different positions in the flow direction along the radial slitting direction. The numerical simulation results show the rotor pressure ratio and efficiency have been significantly improved. After comparing the simulation results of different suction positions, it is proposed that the suction effect in the position where the separation is about to be expanded is the most ideal. According to the results of numerical simulation, literature [11] proposed that for high subsonic stator blade profiles, suction near or within the separation zone may not be conducive to inhibiting separation, and the best suction position should be located far upstream of the separation zone. In addition, in literature [12-13] the design of aspirated compressor blade profiles are also explored. At present, only the boundary layer suction technology is used as a flow control method to improve the performance of the original design, it has not yet been integrated into the design system to form a complete aspirated design method and complete the design of an adsorption fan/compressor from scratch. In view

of this, in this paper, a relatively complete design system of the aspirated compressor is established and based on this system an aspirated compressor with a stage pressure ratio of 3.51 and a load factor of over 0.6 is designed.

DESIGN AND ANALYSIS METHODS

Design and analysis tools

The tools used in the quasi-three-dimensional design in this paper are the S2 streamline curvature code and the MISES code [3]. The MISES code can be used to calculate the flowfield of the S1 surface for the analysis problem, and it can also be used for the blade design for inverse problems that is, the blade profile geometry can be obtained by specifying or modifying the pressure distribution on the blade profile surface. In this code there is a suction module, which can easily modify the key suction design parameters, so it is especially suitable for the design of aspirated compressor blade. The optimization of the aspirated blade profile suction scheme adopts the self-developed aspirated blade profile optimization system. In this system, the suction amout and suction position are optimization variables, differential evolution algorithm based on natural evolution is adopted, and blade profile loss as an objective function, quasi-three-dimensional suction for every sample is calculated taking MISES code and its suction module as the flow field evaluation system, and finally the global optimal suction scheme is obtained. The flow chart of the specific suction scheme optimization is shown in Figure 1. The 3D flowfield analysis tool is based on the commercial software NUMECA/Harmonic module. The nonlinear harmonic method (NLH) has the characteristics of unsteady time-averaged property to some extent, and has a strong ability to capture the interference between stages. The order of the harmonic can be controlled to achieve a balance between the calculation time and accuracy[14].

Design Process

The core of the whole design process is the iterative calculation of the S1/S2 flow surface. The specific design flow chart is shown in Figure 2. In the process of blade profile design, three typical blade sections of hub, middle and tip are taken for analysis of the rotor and stator. After the design goal is determined, the inlet and outlet parameters of each S1 flow surface are first calculated by the S2 flow surface, and the parameters are used for initial modeling. At the same time, the Xfoil code [15] is used to fine-tune the initial blade profile so that the initial blade profile basically meets the aerodynamic requirements. Then MISES code is used to calculate the non-viscous S1 flow surface with the adjustment of the thickness of the flow surface to obtain the optimized blade profile. Finally, analysis with the boundary layer is carried out, and the optimal combination of suction amount and suction position is found by using intelligent optimization algorithm.

If the boundary layer separation cannot be suppressed, it is necessary to return to the inviscid design stage to redesign the airfoil. When all S1 calculations are completed, the calculated aerodynamic parameters of each S1 shall be compared with the corresponding streamline calculation results of the S2. If the maximum error is higher than a set value, the flow surface of S2 shall be recalculated based on the new airflow parameters, until the error meets the requirements. After completing the blade profles design of the typical cross-section of each blade row, the blade profiles shall be stacked into a three-dimensional blade, and the commercial software NUMECA/Harmonic is used to check the full three-dimensional time-averaged flow field. If it is found that the total performance of the compressor does not meet the design goal, it is necessary to return to the design according to the three-dimensional flow field results until a satisfactory design scheme is obtained.

RESULTS AND DISCUSSION

Based on the aspirated compressor design method established above, a highly-loaded aspirated compressor is designed. Its main design parameters are: massflow 36.5kg/s, stage pressure ratio 3.5, isentropic efficiency 86.5%, speed 18kr/min, load coefficient 0.62.

Quasi-three-dimensional design results

The suction scheme after the final iteration is given in Table 1, in which the suction amount is the percentage of the relative inlet flow, and the suction position is the ratio of the distance (X) from the suction slot to the leading edge of the airfoil along the airfoil chord direction to the airfoil chord length (C). For space reasons, only the design results of several typical rotor and stator sections are analyzed in detail

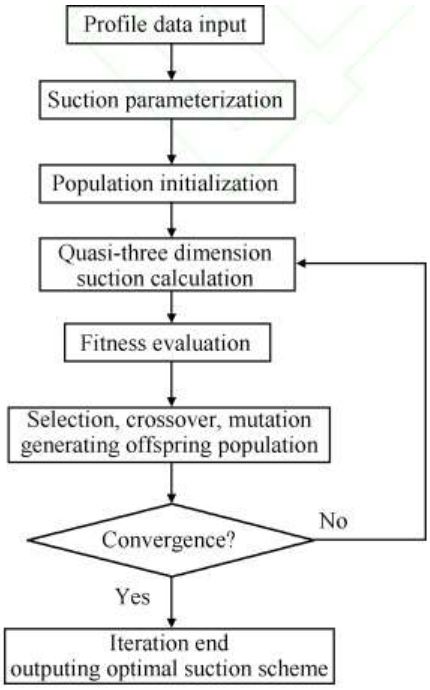

Fig. 1 Flow diagram of suction scheme optimization

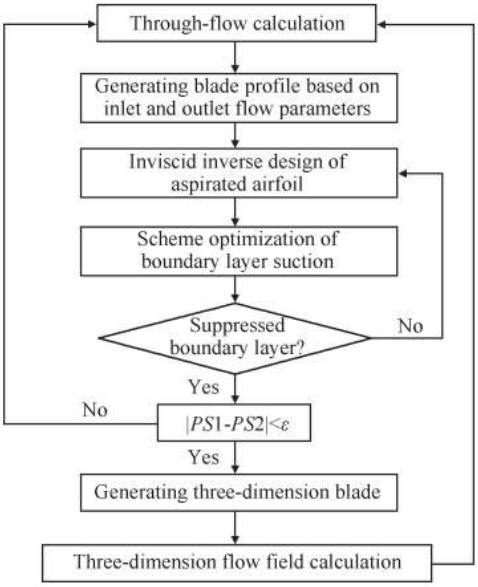

Fig. 2 Flow diagram of aspirated compressor design

Item	Rotor			Stator		
Blade height location	Hub (10%)	Mid (60%)	Tip (90%)	Hub (10%)	Mid (50%)	Tip (90%)
Suction mass	None	1%	1.6%	1.1%	0.5%	0.8%
Suction location	None	40%~42%	42%~45%	45%~47%	45%~47%	46%~48%

Table 1 Suction mass and location at different span

（1）Design of the hub section of the rotor

Figures 3 and 4 show respectively the surface isentropic Mach number distribution and Mach number contour of the section of rotor hub. The Mach number of this section at the inlet is 0.77, which accelerates to about 0.95 at the leading edge, and then slowly and uniformly decreases to the trailing edge along the suction surface.

Because there is no shock wave in the channel, there is almost no separation of the flow and no suction. Considering that the designed turning angle is far beyond the conventional one, in order to keep the control loss at a lower level, the value of passage expansion degree is more conservative, and the total pressure ratio required by the blade root section is mainly achieved through high-speed rotation at the design speed without relying on shock wave pressurization. According to the velocity triangle, it can be judged that a very high circumferential velocity occurs to the outlet of the rotor hub, which in turn causes the inlet Mach number of the downstream stator blade row to be much higher than that of the conventional aerodynamic design.

（2）Design of the tip section of the rotor

The rotor tip section surface isentropic Mach number distributions are shown in Figures 5 and 6. The Mach number at the inlet of the section is 1.51, which is reduced to about 1.47 through the pre-compression section, and then rapidly reduced to about 0.75 through the passage shock wave, and the pressure recovery section is formed from the shock wave to the trailing edge.

The optimized suction position is 3% chord length downstream of the shock wave, and the suction amount is 1. 6% of the inlet flow rate. Because the total pressure ratio needed to be achieved at the S2 design tip is not enough to be pressurized only by the shock wave, a subsonic diffuser section of more than 20 ° downstream of the shock wave is designed.The shape factor (H) distribution under this section is shown in Figure 4(b). The shape factor (H) distribution for this section is shown in Figure 4 (B). The suction surface shape factor remains horizontal in front of the shock wave, and increases rapidly to 7.5 at the shock wave position, forming a local peak. The suction completely suppresses the growth of the downstream boundary layer, and the shape factor is controlled at a low level until the trailing edge. According to the judgment standard of 2.76 ± The shape factor is kept within the separation limit except near the shock.

（3）Design of the hub section of the stator

The stator root section surface isentropic Mach number distributions are shown in Figures 7 and 8. The inlet Mach number of this section is 1.21, and the flow accelerates to about 1.35 at the leading edge point.Similar to the rotor tip section, the flow also passes through a small pre-compression section in the leading edge section to reduce the wave front Mach number, and then rapidly reduces to about 0.7 through the passage shock, and then enters the pressure recovery section of deceleration and diffusion, and the Mach number slowly reduces to about 0.55 at the trailing edge. The tendency of the suction side boundary layer to thicken by suction at 45% chord is not significant, and it can be seen from the shape factor distribution in Fig. 5 (B) that the shape factor remains within the separation limit except near the shock.

（4）Design of the mid section of the stator

Figs. 9 and 10 show the surface isentropic Mach number distribution and Mach number contours for the middle section of the stator blade. The inlet Mach number of this section is 1. 15, and it accelerates to about 1. 3 at the leading edge point, and keeps constant in the range of 20% chord length, and then rapidly decreases to about 0. 8 through the channel shock, and there is a relatively gentle pressure recovery region behind the shock. Due to the reasonable design of the blade profile, the blade profile with excellent aerodynamic performance can be obtained only by correcting the surface Mach number distribution several times in the inverse design.Therefore, it is found that only 0.5% of the suction amount is needed to achieve better flow control on the suction surface in the optimization of the suction scheme.

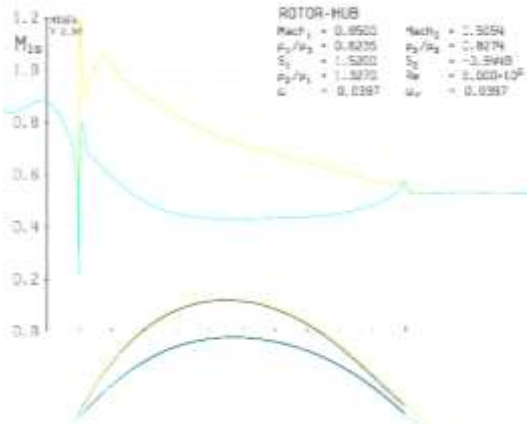

Fig. 3 Mach number distribution at the hub of rotor

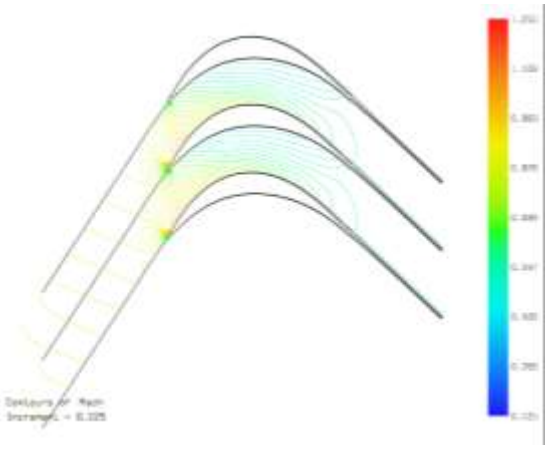

Fig. 4 Mach number contours at the hub of rotor

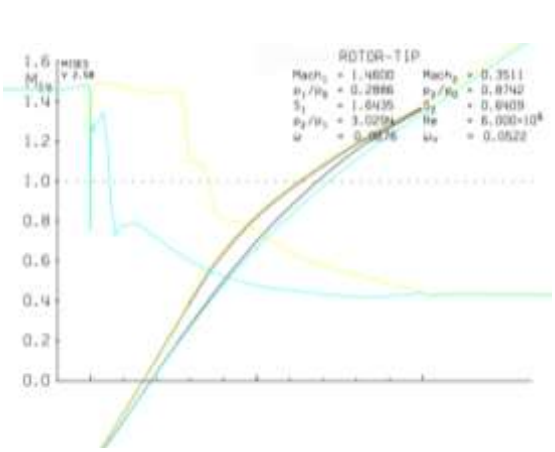

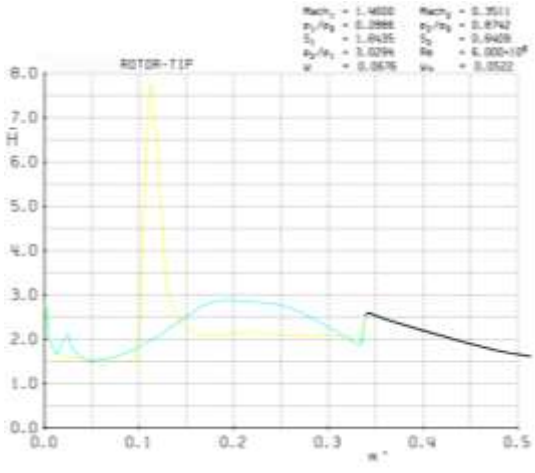

Fig. 5 Mach number distribution at the tip of rotor

Fig. 6 Shape parameter distribution at the tip of rotor

Three-dimensional flow field simulation

（1）Settings of grid and calculation

NUMECA/AUTOGRID5 module is adopted for each blade row to automatically generate O4H grid topology. Since the entire stage three-dimensional flow field calculation is based on the nonlinear harmonic method, the larger value of the circumferential grid number is used to meet the grid requirements of the third-order harmonic [15], finally the rotor and stator grid numbers are 980,000 and 720,000 respectively, 1.7 million in total. NUMECA/Harmonic module is adopted for the computation process, applying Jameson finite volume difference scheme in combination with Spalart-Allmaras (SA) turbulence model to solve Navier-Stokes equation in the relative coordinate system, and second-order precision central difference format is used for spatial discretization. The fourth-order Runge-Kutta method is used to solve iteratively for a time term. In order to speed up the convergence, multi-grid and implicit residual smoothing methods are used. The boundary conditions determine the absolute total temperature, the absolute total pressure, and the inlet airflow angle are given for boundary condtion and , static pressure is given for outlet.

（2）Three-dimensional suction scheme

The three-dimensional suction position of the suction rotor and stator is determined according to the two-dimensional suction scheme optimized for each typical section in the previous paper. For the three-dimensional suction, it is found that the relative suction of 0.7% and 1% can better inhibit the separation for the rotor and stator in the process of a large number of calculations and comparisons of the three-dimensional flow field of the whole stage. The final three-dimensional suction scheme is shown in Figure 11 and Table 2.

（3）Three-dimensional flow field analysis

Figs. 12 to 14 show the time-averaged relative Mach number contours of the entire fan at peak efficiency in the hub, mid and tip sections, respectively. In the whole time-averaged flow field, only a certain scale of separation is formed behind the wave at the stator blade hub, and the flow conditions of other sections are very smooth. The flow field obtained by the time-averaged simulation is not very different from that obtained by the steady simulation of the isolated blade row, which indicates that the initial flow field of the isolated blade row is very close to the final convergence solution of the whole stage, and on the other hand, it also reflects that the interaction between the stages is not as strong as expected due to the successful filling of the wake defect of the upstream rotor blade row after suction. Because the determined stresses better reflect the unsteadiness in the flow field, Figure 15 shows the axial determined stress contours for a typical section of an aspirated rotor at the point of peak efficiency. It is not difficult to see that the determined stress levels in the passage are very low because the suction completely suppresses the development of the boundary layer. The high determined stress area is mainly distributed at the rotor exit, and the determined stress field is more intense closer to the rotor-stator interface, which indicates that the unsteadiness in the rotor flow field is mainly dominated by the potential flow interference propagating from the downstream blade row to the upstream due to the disappearance of the rotor-stator interference source of the wake.

（4）Analysis of entire stage characteristics

The time averaged and steady pressure ratio characteristics of the suction compressor are shown in Fig. 16, and the corresponding efficiency characteristics are shown in Fig. 17. From the figure, it can be seen that the voltage sharing ratio at the design point reaches 3.51, and the time-average efficiency at the design point is 86.82%, which successfully achieves the design goal. Comparing the time-averaged and steady characteristic curves, the differences of peak efficiency and pressure ratio between time-averaged and steady results are only 0. 12% and 0. 003, respectively, due to the fact that the wake defect of the upstream rotor blade row is basically eliminated by suction and the inter-stage interference effect is weak, and the shape and trend of both are basically the same.

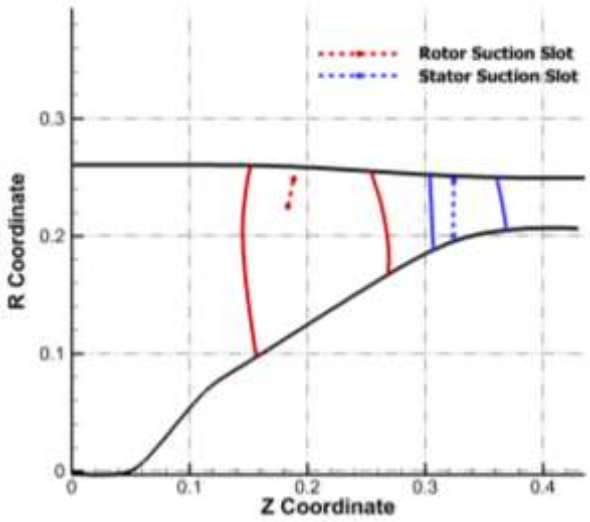

Fig. 11 Three-dimension suction slot of the aspirated compressor

Item	Suction mass	Suction location
Rotor	0.7%	60%–95% (span)
Stator	1%	5%–95% (span)

Table 2 Three-dimension suction scheme of the aspirated compressor

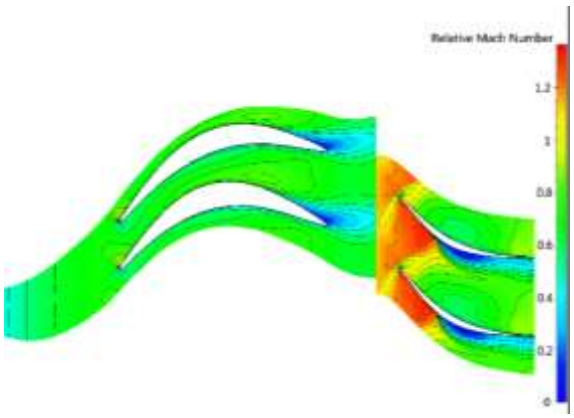

Fig. 12 Relative Mach number contours at the hub of compressor on design point

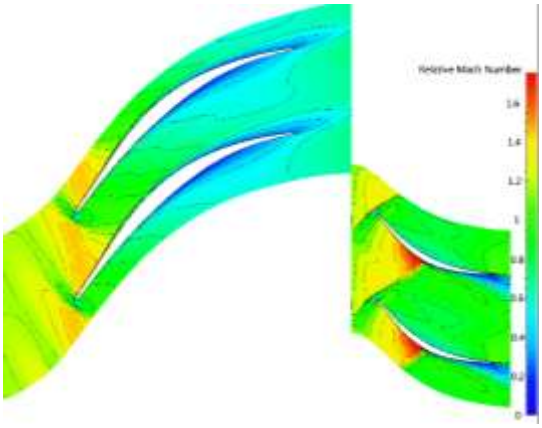

Fig. 13 Relative Mach number contours at the mid of compressor on design point

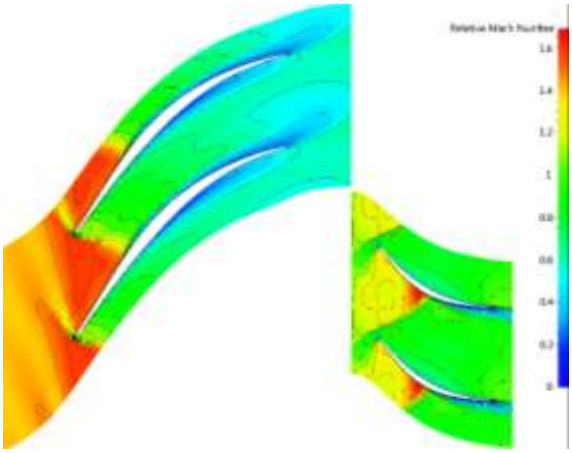

Fig. 14 Relative Mach number contours at the tip of compressor on design point

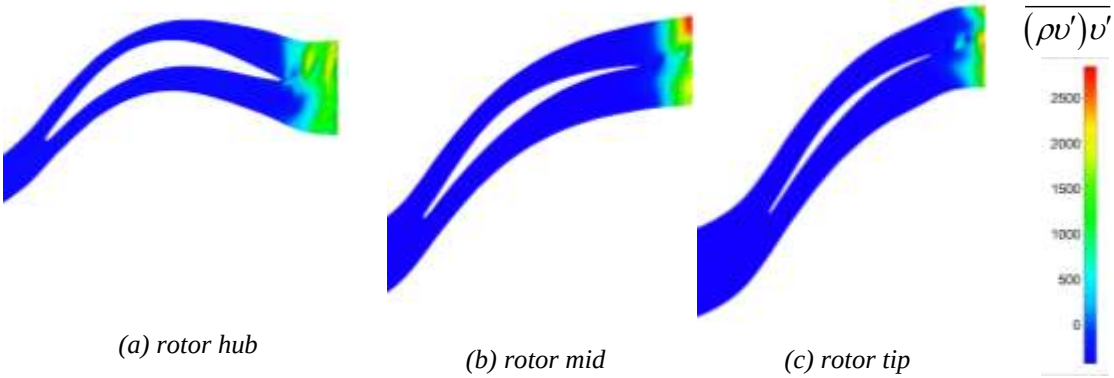

(a) rotor hub *(b) rotor mid* *(c) rotor tip*

Fig. 15 deterministic stress contours for rotor sections at peak efficiency point

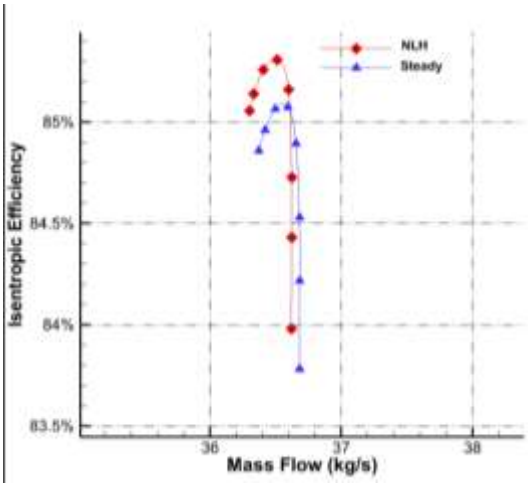

Fig. 16 total pressure ratio characteristic

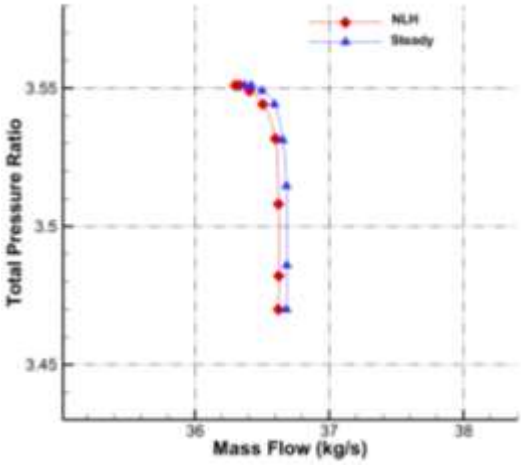

Fig. 17 Efficiency characteristic

CONCLUSIONS

Aspirated technology, which can greatly increase the stage pressure ratio of compressor, is used to study the design system of high-load adsorption compressor and the following conclusions are drawn:

(1) The system can be used to design a highly-loaded aspirated compressor, and a compressor with a load coefficient of more than 0.6 was designed and completed based on the system. The three-dimensional time-averaged flow field calculation based on the nonlinear harmonic method shows that only 1. 7% of the relative suction is used. The stage pressure ratio and efficiency of the adsorption compressor reach 3.51 and 86.82% respectively.

(2) Because the suction successfully eliminates the wake of the upstream rotor blade row, the interstage interaction effect is not strong in such a high load compressor, and the peak efficiency and pressure ratio in the time-averaged and steady characteristic lines are only 0. 12% and 0. 003, respectively, and their shapes and trends are basically the same.

REFERENCES

Kerrebrock J L, Reijnen D P, Ziminsky W S (1997)， et al. Aspirate*d Compressors*. *ASME 97-GT-525.*

Kerrebrock J L (2000). *The Prospects of Aspirated Compressors*. *AIAA 2000-2472.*

Merchant A. (1999)Design and Analysis of Axial Aspirated Compressor Stages. *Cambridge: Massachusetts Institute of Technology*.

Merchant A A, Drela M, Kerrebrock J L, et al. (2000) Aerodynamic Design and Analysis of a High Pressure Ratio Aspirated Compressor Stage. *ASME GT*-2000-619.

Merchant A, Kerrebrock J L, Epstein A H. (2004)Compressors with Aspirated Flow Control and Counter- Rotation. *AIAA 2004-2514.*

Knapke R D, Beach T, Merchant A. (2008)Time Accurate Simulations of a Counter-Rotating Aspirated Compressor. *ASME GT-2008-50877.*

Merchant A. (2005) Experimental Investigation of a High Pressure Ratio Aspirated Fan Stage. Journal of Turbomachinery,127(1),pp.43-51.

Schuler B J. (2006)Experimental Investigation of a Transonic Aspirated Compressor. *Journal of Turbomachinery.127(2),*pp.340-348.

YG, Wang, N Niu, LB Zhao, et al. (2012)The influence of the suction position at the end wall on the separation control of the compressor cascade angle. *Propulsion technology,*

H Zhou, QS Li, YJ Lu. (2004)Numerical experiment exploration of suction air from rotor blades of transonic fan rotor, *Journal of Aerospace Power, 19(3),*pp.408-412.

ZG Zhou, CB Wang. (2007)Research on the calculation and simulation of aerodynamic performance of adsorption compressor cascade. *Journal of Aerospace Power ,2(12)* ,pp.2036-2042.

FX Lan, BH Zhou,DW Liang. (2010) Research on blade profile design technology of adsorption compressor. *Journal of Aerospace Power, 23(12): 2296-2301.*

FX Lan.Research on design technology of adsorption compressor. (2007) Nanjing: Nanjing University of Aeronautics and Astronautics.

L Wang, B Liu. (2012)Calibration analysis of nonlinear harmonic method in counter-rotating compressor. *Journal of Aerospace Power, 27(7),*pp.1448-1455.

Drela M， Youngren H. (2001)XFOIL 6. 94 User Guide.*Cambridge: Massachusetts Institute of Technology*.